https://doi.org/10.1142/9789811280184_0009

Chapter 9

Beam Collimation, Dump and Injection Systems

Chiara Bracco and Stefano Redaelli

CERN

High-performance beam collimation, injection and beam-disposal systems are essential for operating efficiently and safely modern hadron accelerators at the beam intensity frontier. In particular, the superconducting environment in colliders that work in the multi-TeV energy regime poses specific challenges that need to be addressed through optimized designs and operational schemes. The upgraded collimation system for HL-LHC is presented, addressing both the performance with protons and heavy-ion beams, and taking into account recent changes of the upgrade baseline. The upgrades applied to improve the reliability of the fast pulsed kickers of the injection and extraction systems are also addressed together with the new advanced designs and cutting-edge materials of the different collimators and dumps to cope with the unprecedented energy of the HL-LHC beams.

1. The HL-LHC beam stored-energy challenge

Figure 1 shows the stored beam energy for a selection of past, operating and future hadron and lepton machines. Handling beams at the beam stored-energy frontier poses obvious challenges in superconducting environments like the ones of the LHC and of its high-luminosity upgrade, HL-LHC. During its Run 2 (2015–2018) at 6.5 TeV, the LHC achieved successfully regular, high-efficiency operation close to its design value of 362 MJ [Brüning *et al.* (2004)]. This is about two orders of magnitude above the previous state-of-the-art achieved by the Tevatron (see Fig. 1). The LHC performance benefited from the high-performance multi-stage collimation system [R. W. Assmann *et al.* (2006)] but a further step is needed to meet the HL-LHC ambitious goals.

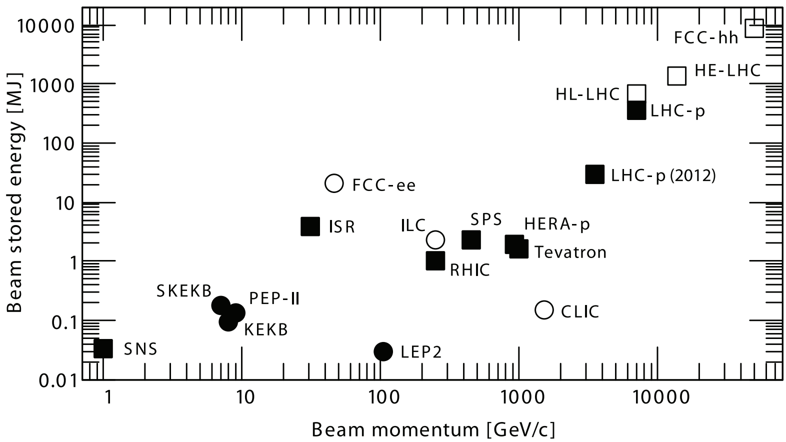

Fig. 1. Livingston-like plot of the stored beam energies for hadron (squares) and lepton (circles) accelerators. Filled symbols are used for past or operating machine and empty symbols indicate future accelerators. *Courtesy R. Aßmann.*

Injection and extraction are among the most critical systems in the LHC. The magnets used in these systems are fast-pulsed kickers operating at very high voltage. In case of a failure, high intensity beams can be mis-kicked and induce quenches in several superconducting magnets and, in the worst case, even damage the machine and the experiments. Passive protection elements are installed downstream of the injection and extraction kickers to intercept mis-kicked beams and shadow the machine aperture in order to reduce the energy deposited on the magnets and prevent any damage.

The HL-LHC upgrade project foresees doubling the stored beam energy with beams up to 5 times brighter, leading to unprecedented challenges for beam collimation and machine protection systems. A number of upgrades of the LHC systems were conceived in order to handle efficiently and safely beam stored energies up to 700 MJ at 7 TeV throughout the operational cycle, achieving the target performance with sufficient margins. Note that the injected stored energy per train increases from about 2.4 MJ to 4.8 MJ. The HL-LHC also operates as a heavy-ion collider with nearly double intensity compared to Run 2 [Coupard *et al.* (2016)].

2. The HL-LHC upgrade of the injection system

The LHC ring has an eight-fold symmetry with 8 insertion regions (IRs) dedicated to the four main experiments (ATLAS [ATLAS Collaboration

(2008)] in IR1, ALICE [The ALICE Collaboration (2008)] in IR2, CMS [CMS Collaboration (2008)] in IR5 and LHCb [The LHCb Collaboration (2008)] in IR8), to the off-momentum (IR3) and betatron (IR7) collimation systems, to the radio-frequency system (IR4), to the beam dumping system (IR6). IR2 and IR8 also house the injection systems for clock-wise Beam 1 and anti-clock-wise Beam 2, respectively. The injection takes place about 200 m upstream of ALICE and LHCb experiments [Brüning *et al.* (2004a)]. The beam to be injected into the LHC passes through five horizontally deflecting steel septum magnets (MSI) and four vertical deflecting kickers (MKI) steer the injected beam onto the LHC closed orbit. The kickers pulse at 25 kV and operate at $\sim 10^{-11}$ mbar to minimise the risk of flashovers. The full magnetic pulse consists of a 900 ns rise time, a flattop of 7.87 µs and a fall time of 3 µs. Uncontrolled beam losses resulting from MKI errors (missing pulses, erratic, partial, badly synchronized or wrong kick strength) could result in serious damage to the downstream equipment. In particular, the beam could directly hit the superconducting separation dipole D1, the triplet quadrupoles magnets near the ALICE and LHCb experiments or any other exposed machine aperture around the ring. In addition, particle showers, generated by proton losses, could damage components of the detectors, which are close to the beam pipe. Precautions must therefore be taken against damage and magnet quenches and, to that purpose, a dump (TDIS) is installed at about 90° phase advance from the injection kicker to protect the downstream components in case of MKI malfunctions and timing errors.

2.1. *Injection kicker*

The injection kicker magnets consist of U-core ferrite cells between two high voltage (HV) conducting plates. Extruded ceramic tubes (99.7% alumina), with 24 screen conductors lodged in its inner wall, are placed within the aperture of each MKI magnet [Ducimètiere *et al.* (2003)]. A set of toroidal ferrite rings is mounted around each end of the alumina tube, outside of the magnet aperture to damp low-frequency resonances. To ensure reliable operation of the MKI magnets, the temperature of the ferrite yokes must not exceed their Curie point, which is ∼125°C. Above this temperature, the magnetic properties of the ferrite are compromised, and the beam cannot be injected. The MKI kickers installed in IR2 and IR8 for the first LHC run encountered a number of issues that affected operation [Barnes *et al.* (2018)]. These include beam-induced heating and electron cloud related vacuum pressure rise, which caused, in some cases, electrical breakdowns and surface flashovers. The conditioning process of the alumina tubes with beam was slow, requiring approximately 300 hours, and this could strongly affect beam operation in particular in case of replacement of a magnet in the middle of a run. As a mitigation to this problem, a 50 nm thick Cr_2O_3 coating [Barnes *et al.* (2017)], applied by magnetron sputtering to the inner part of the alumina tubes, allows a rapid reduction of the dynamic vacuum and a significantly faster conditioning with respect to the original design. The power deposition in the MKI for operation with HL-LHC beams is expected to be a factor of four higher than for the LHC, which would be unacceptably high for the original magnet design and would require cooling the ferrite yokes. Impedance studies show that it is possible to redistribute the beam induced power deposition, from the yoke to the upstream ferrite rings by modifying the geometry of the metallic cylinder that provides capacitive coupling to the open ends of the screen conductors. The rings can then be much more easily cooled down than the yokes since they are not pulsed at high voltage (Fig. 2). Studies shows that an active water cooling system just of the rings is sufficient to keep the temperature of the full magnet below 100°C also for HL-LHC beams [Vlachodimitropoulos *et al.* (2018)]. A complete prototype with Cr_2O_3 coated chambers, upgraded beam screen with active cooling of the ferrite rings, the so called "MKI-cool" will be installed and tested in the LHC during the 2022–2023 winter stop for the final validation before launching the upgrade of the full series.

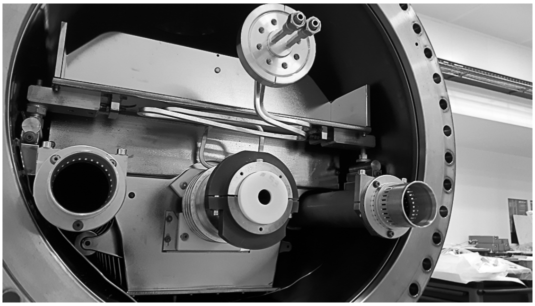

Fig. 2. Detail of the cooling system installed around the upstream ferrite rings of the MKI-cool.

2.2. *Injection Protection Dump*

The original injection protection dump consisted in a movable two-sided vertical absorber composed by two, 4.185 m long jaws accommodating blocks of graphite, aluminum and copper alloy CuCr1Zr. This design proved to be affected by several anomalies including outgassing, vacuum spikes, structural damage of the beam screens and elastic deformation of the jaws due to beam induced RF heating during the first years of the LHC operation [Lechner *et al.* (2016)]. A new improved design in terms of mechanics, robustness, reliability, setup accuracy, impedance and operational aspects was conceived for HL-LHC. The new injection dump [Carbajo Perez *et al.* (2021)] (Fig. 3), called TDIS, consists of three modules of equal length (each 1.6 m long) hosting different materials. The first two modules are made of low-Z graphite absorbers blocks to dilute the beam while the last module is constituted of a sandwich of higher-Z materials (Ti_6Al_4V and CuCr1Zr) to partially absorb and efficiently attenuate the particle showers from the low-density upstream blocks. The shorter jaws and the improved mechanics allows a more precise beam-based alignment, less prone to deformation due to beam induced heating and less sensitive to mechanical offsets and angles. The correct positioning of the TDIS jaws around the beam is indeed vital for machine protection. Each jaw of each module is independently movable in order to be aligned with respect to the circulating beam. Redundant position measurements are performed and checked via the Beam Interlock System. The upgraded systems were installed in both injection regions already during the Long Shutdown 2 (LS2); this will allow to probe their performance with higher intensity beams well in advance before the start of HL-LHC operations.

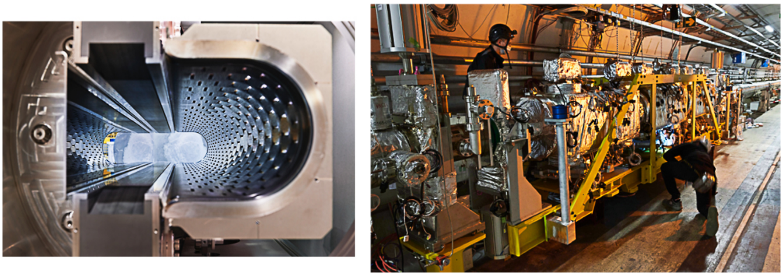

Fig. 3. The cross-section of one of the new TDIS modules is shown on the left: the graphite jaws have to intercept any vertically mis-kicked beam while the counter-rotating beam circulates unperturbed, in the same vacuum tank, to the side of the jaws. The TIDS installed in IR8 of the LHC is also shown on the right.

3. The HL-LHC Upgrade of the Beam Dump System

The LHC Beam Dump System (LBDS) [Brüning *et al.* (2004b)] is installed in IR6 and has to fast-extract the beam in a loss-free way and to transport it to an external dump (TDE), which is located approximately 650 m downstream of the extraction point. This requires a particles-free gap, in the circulating beam, for the rise time of the field of the fifteen fast-pulsed extraction kicker magnets (MKD) which deflect the beam horizontally into a set of fifteen Lambertson septum magnets (MSD). The septa deflect the beam vertically out of the LHC ring into the extraction channel up to the TDE. Ten dilution kickers (four horizontal MKBH and six vertical MKBV), installed ∼80 m downstream of the MSD, dilute the extracted beam on the front face of the dump over a quasi-elliptical shaped area. The dilution and the long drift allow minimizing the local energy density on the dump. The synchronization between the beam-free abort gap and the field rise-time is ensured by a highly reliable timing system. Nevertheless, several failure modes exist in the synchronization system and the kicker switches which could led to an asynchronous dump, in which several hundreds of bunches could be swept across the LHC aperture by the rising kicker field. Two absorbers, a fixed block (TCDS) and a mobile diluter (TCDQ), are installed immediately upstream of the MSD and the Q4 superconducting quadrupole magnets in order to protect them from damage in the event of an asynchronous firing of the MKD kickers. No or minor modifications are required for both the TCDS and TCDQ to make them compatible with HL-LHC beams operations.

3.1. *Extraction and dilution kickers*

The fast-pulsed kicker magnets which are employed in the extraction and dilution system, operate at several tens of kV and can be subjected to spurious firings and flashovers. In case of loss of synchronisation between the RF system and the abort gap, or if one of the kickers undergoes a spontaneous firing, an asynchronous beam dump occurs. A fault of the MKBs would instead result in a reduced dilution at the dump front face with a consequently higher energy deposition density. The LBDS controls include a re-triggering system which, if one kicker pulses spontaneously, detects the pulse and fires all the remaining magnets. The detection of an erratic and a fast reaction of the system, within specified limits, is fundamental to minimise the effects of the failure. In order to deal with the new HL-LHC beam parameters and to ensure the highest machine availability, several consolidation items were put in place to reduce the occurrence of erratics and limit their consequences [Allonneau *et al.* (2018); Ducimètiere and Senaj (2018); Magnin *et al.* (2019)]. In particular, a third capacitor was added in the high voltage generator to lower the operational voltage and hence reduce the probability of self-trigger. New power trigger modules were implemented to increase the trigger peak current at the HV switches and reduce the stress on the switches. The re-triggering line length was shortened to reduce the reaction time to self-triggers events. The related diagnostics was also upgraded and a Spark Activity Monitoring (SAM) systems for early detection of sparking activity inside the HV generators, before degradation that could result in a self-trigger, was deployed.

3.2. *Dump*

Each LHC dump consists of a graphite core housed in a stainless-steel tube. The core is composed of different graphite segments, comprising six 70 cm-long isostatic Sigrafine© blocks (1.7 g/cm^3) and a 350 cm long segment made of 2 mm-thick Sigraflex© sheets (1.1–1.2 g/cm^3) which are supported by a few cm-thick extruded Graphite plates. The dump core has to be kept under a slight over pressure (100–200 mbar) of Nitrogen (N_2) to avoid oxidation and mass loss when heated up by the beam. During the first two LHC runs, a problem with beam induced vibrations and displacements was discovered which led to N_2 leaks at the different gaskets in the connection line. The vibrations were attributed to the lateral leakage of particle showers from the graphite core (mainly the Sigraflex© segment), which deposit a non-negligible amount of energy in the stainless-steel shell within the beam dump event. This rapid heating results in a highly dynamic response of the whole dump structure. In order to mitigate the vibration effects and avoid any risk of contaminating the LHC ultra-high vacuum (UHV), several modifications were put in place during LS2 [Martin *et al.* (2021)]. The core, which is kept in N_2 atmosphere, was disconnected from the LHC vacuum line and was suspended by a cradle-like support (Fig. 4) to absorb the vibrations and prevent as much as possible permanent longitudinal drifts of the system. Upgraded 3D forged Ti6V4Al alloy windows were installed at the entrance and exit of the dump and an additional UHV Ti window was placed at the end of the vacuum line. Despite the applied modifications, new upgraded dumps will be needed to cope with HL-LHC standard beams during nominal operation ($\sim$52% of initial intensity, i.e.

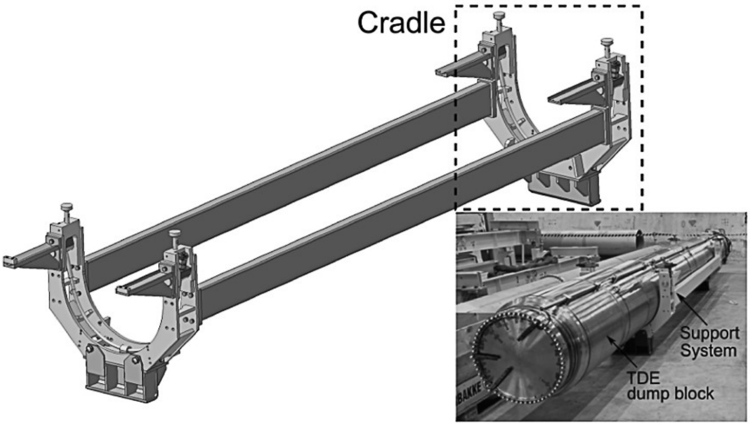

Fig. 4. 3D view of the new dump support frame with cradles at each end. The inset photo shows both upgraded dump blocks assembled in their support systems prior to installation. *Courtesy of J. Maestre*

3.3×10^{14} protons, dumped at the end of each fill) and in case of MKB failures (two missing horizontal MKBs as worst failure case scenario). The experience gained during the first years of beam operation in Run 3 with the present dumps will provide fundamental inputs and information for the design of the new dumps. Characterisation studies, the autopsy of the operational beam dumps and beam-impact tests in the HiRadMat facility allowed some preliminary information to be collected concerning possible materials for the dump core. In particular, Sigraflex© or C/C composites were identified as candidates for the low density sector while CFC should replace the extruded Graphite plates in the high density part. Further tests are needed to qualify the long-term resistance to beam impacts and studies are being performed to finalise the design and the choice of the vessel material (stainless steel or Ti).

4. The HL-LHC upgrade of the LHC collimation system

4.1. *Introduction*

The backbone of the HL-LHC collimation system will remain, as for the current LHC, the betatron and momentum multi-stage cleaning systems. Each system relies on the multi-stage transverse hierarchy illustrated in Fig. 5. In the following, circulating beam particles with transverse

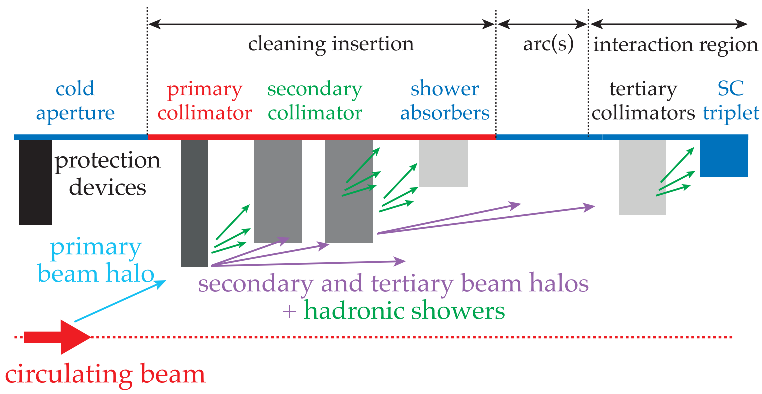

Fig. 5. Schematic illustration of the LHC multi-stage collimation cleaning system. Primary and secondary collimators (darkest grey) are closest to beam and are made of robust carbon-fibre-carbon composites. Shower absorbers and tertiary collimators (lighter grey) sit at larger apertures and are made of a tungsten alloy to improve absorption, in the shadow of protection devices (black). Collimators of different families are ordered in a pre-defined collimation hierarchy that must be respected to ensure the required system functionalities.

amplitudes within, say, 3–4 σ of the RMS beam distribution are referred to as *beam core* as opposed to the ones above this value that are referred to as *beam halo* or *halo particles*. The border between these two regimes is somehow arbitrary. Core particle contribute significantly to the collider's luminosity production while halo particle do not and are subject to cause potentially detrimental beam losses. The multi-stage collimation system constrains the maximum betatronic and off-momentum amplitudes of halo particles with sufficient margins to the accelerator aperture to ensure a safe operation.

Primary collimators (TCPs) intercept the beam losses in case of diffusion, beam instabilities or failures experienced by the circulating beam. A very efficient halo cleaning at the energies of interest requires several secondary (TCS) collimators and shower absorbers (TCLA) to suppress the large-amplitude beam halos and to safely dispose of the energy deposited by the electromagnetic and hadronic showers produced by the interactions of halo particles with the collimator materials. Tertiary collimators (TCTs) are part of the betatron system and are located in front of the aperture bottlenecks at the super-conducting (SC) triplet magnets that provide the final focusing close to the experiments. In addition, the high-luminosity experimental regions need a physics debris collimation scheme to safely dispose of the collision products. These different collimation schemes are already part of the LHC systems and will be upgraded for HL-LHC. Injection protection and dump devices discussed above are also part of the transverse hierarchy as shown in Fig. 5.

The collimation upgrades required for HL-LHC are [Redaelli *et al.* (2020)]:

(i) Improved betatron collimation cleaning around IR7, particularly for heavy-ion operation.
(ii) Reduction of the collimator-induced impedance to allow operation with higher-brightness beams.
(iii) Improved protection of the dispersion suppressors (DSs) around ALICE in view of the luminosity upgrade for ion operation.
(iv) Improved physics debris collimation around ATLAS and CMS to enable a 5 times larger peak luminosity (levelled) than the LHC design.
(v) Improved tertiary-halo collimation around the high-luminosity experiments.

The active halo control of the high stored-energy beams, for example through hollow electron beams [Redaelli *et al.* (2021a)], is no longer part of the HL-LHC baseline however it is still pursued as a potential future upgrade beyond the scope of the HL-LHC project.

The upgrade strategy to fulfill these complex requirements was to stage the key collimation upgrades in two phases. The first phase started in the LHC second long shutdown (LS2, 2019–2021) with the deployment of:

- the collimation cleaning upgrades around IR2 (2 TCLD collimators);
- the first phase of the low-impedance upgrade of the system, involving the installation of 8 new secondary collimators (TCSPM) and 4 primary collimators (TCPPM) in IR7;
- the improvement of the protection of warm magnets in IR7 against radiation effects by means of two new passive absorbers (TCAPM);
- the crystal collimation for ion beams in IR7.

The completion of the upgrade is planned for the LS3 (2026–2029), with the installation in IR7 of 10 additional low-impedance secondary collimators and possibly 2 TCLD in the DS, with the deployment of all the IR1 and IR5 upgrades (28 movable collimators and 12 fixed-aperture masks). The complete list of collimators that will be part of the HL-LHC collimation system is given in Table 1. Including damage protection elements, details

Table 1. List of the HL-LHC collimators, including their abbreviated names, plane (H = horizontal, V = vertical, S = skew), the number of installed units, the material (CFC = carbon-fibre composite, W = heavy tungsten alloy (Inermet180), MoGr = molybdenum-graphite, CuCD = copper-diamond) and the operational openings in collision in units of beam σ for p-p operation at $\beta^{\star} = 15$ cm.

Functional type	Name	Plane	Num.	Mat.	Setting[a]
Primary IR3	TCP	H	2	CFC	17.7σ
Secondary IR3	TCS	H	8	CFC	21.3σ
Absorber IR3	TCLA	H, V	8	W	23.7σ
Passive absorber IR3[c]	TCAP	–	4	W	–
Primary IR7	TCP	H, V, S	2	CFC	6.7σ
Primary crystal IR7	TCPC	H, V	4	Si	6.5σ
Low-impedance primary IR7	TCP	H,V	4	MoGr	6.7σ
Secondary IR7	TCS	H, V, S	4	CFC	9.1σ
Low-impedance secondary IR7	TCS	H,V,S	18	MoGr	9.1σ
Absorber IR7	TCLA	H, V	10	W	12.7σ
Passive absorber IR7[c]	TCAP	–	8	W	–
Passive absorber mask IR7[c]	TCAPM	–	2	Steel	–
Dispersion suppressor IR7	TCLD	H	2	W	16.6σ
Dispersion suppressor IR2[c]	TCLD	H	2	W	30σ
Tertiary IR8	TCT	H, V	8	W	43.8σ
Tertiary IR2	TCT	H, V	8	W	17.7σ
Tertiary IR1/IR5	TCT	H	8	CuCD[d] or W	10.4σ
Tertiary IR1/IR5	TCT	V	8	W	10.4σ
Physics debris IR1/IR5	TCL	H	12	W	14σ
Physics debris IR1/IR5 mask	TCLM	–	12	Cu / W	–
Dump protection IR6	TCDQ	H	2	CFC	10.1σ
	TCSP	H	2	CFC	10.1σ

[a] A reference proton emittance of 2.5 μm has been used for a 7 TeV beam energy.
[b] Only used for operation with heavy-ion beams.
[c] Non movable, fixed-aperture collimators or masks.
[d] CuCD is no longer part of the HL-LHC baseline following the decision in Sep. 2022 to build all TCTs in Inermet180. The possibility to deploy it as future upgrade of the HL-LHC is being considered.

of the collimator designs can be found in [Redaelli *et al.* (2020); Carra *et al.* (2014); Dallocchio *et al.* (2011); Valentino *et al.* (2017)].

4.2. *The new collimation in the high-luminosity regions*

The magnetic elements and collimator layout around the ATLAS experiment in IR1 are shown as a function of the longitudinal coordinate in Fig. 6 for the Beam 1. The IR5 layouts are equivalent. Two pairs of horizontal and vertical tertiary collimators are needed in front of the Q6 magnets (labelled "TCT6") and of the triplet magnets ("TCT4") in order to protect

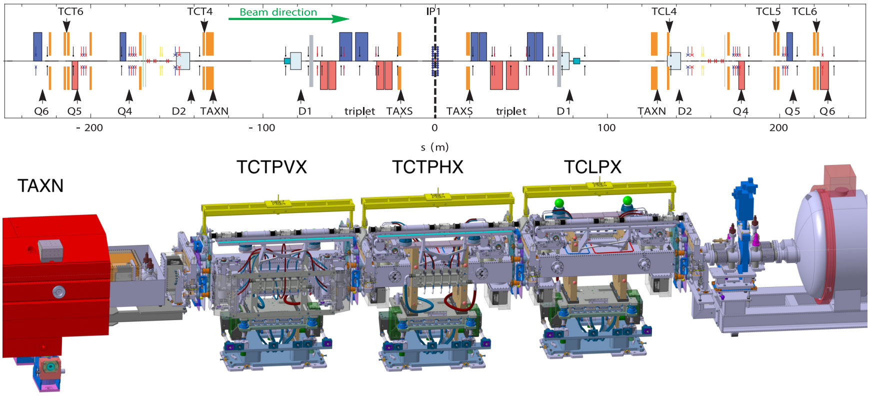

Fig. 6. Layout around ATLAS for the HL-LHC optics version 1.3 (top graph) and 3D drawing of the novel, 2-in-1 collimators called TCTPVX, TCTPHX and TCLPX (bottom). Courtesy of R. Bruce and J. Oliveira, CERN.

adequately the interaction region magnets from incoming beam losses. On the outgoing beam, three movable physics debris collimators (TCL) and three fixed-aperture masks are needed to avoid quenches and radiation damage from the collisional debris losses in high-luminosity proton collisions. A new, two-beam design concept has been conceived to install the required devices in the tight space of the beam recombination region around the experiments, where the beams share the same vacuum pipe (Fig. 6).

During LS2, the ALICE experiment was upgraded to be compatible with a peak luminosity up to 7 times higher than in Run 2, up to at least 7×10^{27} cm^{-2}s^{-1}. This entails specific challenges that are discussed in Chapter WP2. Ultraperipheral electromagnetic interactions between the opposing ion beams, in particular the bound-free pair production (BFPP), limits the achievable peak luminosity in absence of improved collimation to dispose of the products that emerge from the collision points. During LS2, two TCLD collimators were added around IP2, in two connection cryostats in cell 11 at both sides of IR2, to efficiently remove this limitation. A photograph of the installed collimator in shown in Fig. 7.

4.3. *The new betatron collimation system*

The collimation cleaning upgrades are primarily required by the increased risk of quenches from off-momentum losses around IR7. These regions, called dispersion suppressors (DS), are the first part of the arcs downstream of IR7 where the dispersion function starts rising. Particles that

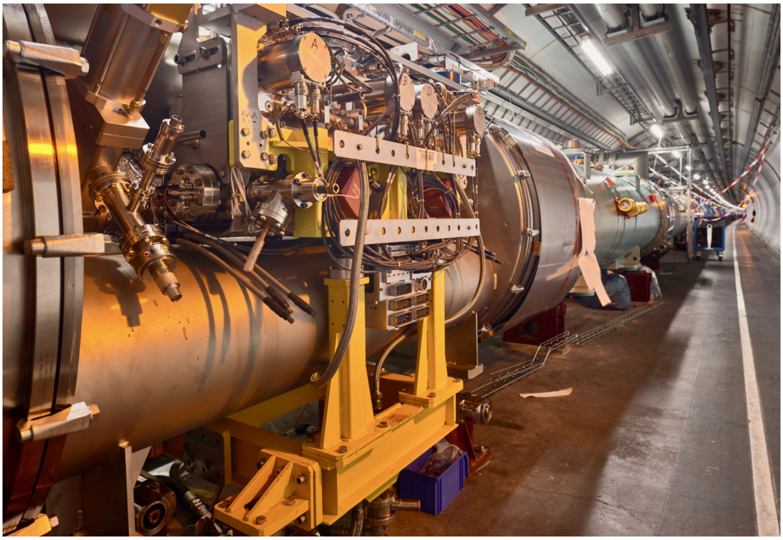

Fig. 7. Photograph of a TCLD collimator installed in the connection cryostat around IR2 (July 2020, Courtesy of M. Brice, CERN).

leak out of IR7 with modified rigidity after the interaction with the betatron collimators, follow perturbed trajectories — the dipole magnets act on them as powerful spectrometers — and risk to be lost locally, possibly causing quenches. This would result in costly downtime and reduced HL-LHC availability. These losses represent the primary collimation cleaning limitation of the present system, both for proton and heavy-ion beams, i.e. these are the locations of the accelerator with the largest losses in superconducting magnets from collimation leakage.

Various solutions were studied as part of HL-LHC to mitigate risk of quenches in the DS magnets. The baseline upgrade relied on adding collimators called TCLDs in the cold region. The space to add this collimator can be made by replacing a standard, 15 m-long LHC dipole with two shorter, 11 T dipoles. One TCLD per IR7 dispersion suppressor would be used, which requires a total of 4 new 11 T magnets. Losses simulated at 7 TeV for the configurations without and with TCLDs are shown in Fig. 8. This upgrade was initially planned to take place in LS2, driven by the upgrade of the ion beam parameters, however it was deferred because of delays with the 11 T dipoles. This is not an immediate concern for proton beam operation as Run 3 will not reach the design HL-LHC parameters yet. The HL-LHC target ion beam parameters will instead be achieved in

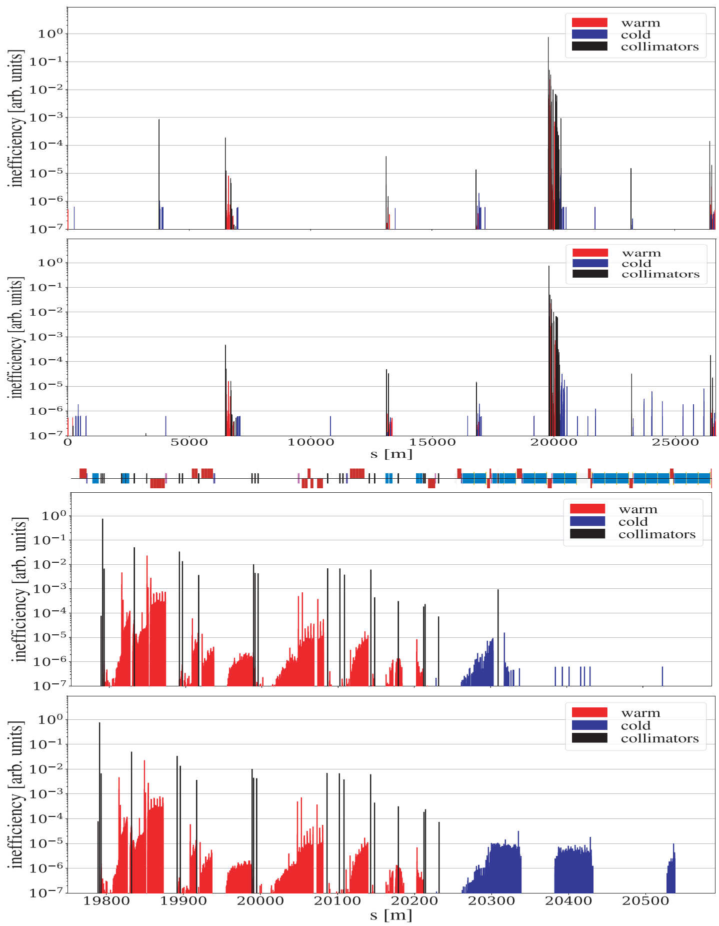

Fig. 8. Simulated loss maps for protons at the HL-LHC, at 7 TeV with 15 cm $\beta^\star$. Top: full ring, with and without TCLD collimators; Bottom: IR7 and its DS, with and without TCLD collimators. Courtesy of B. Lindstrom, CERN.

Run 3. It is important to note that collimation cleaning for ion beams will be improved by the deployment of crystal collimation discussed in the next section that was pursued in WP5 as schedule-risk mitigation for the 11 T program.

Needs for the 11 T dipoles for proton operation in Run 4 will be studied during Run 3 to decide if this upgrade should be deployed. In particular, it is planned to test with beam the quench behaviour of the present dispersion suppressor magnets: this is identified as a critical input for future upgrades based on 11 T magnets. Other critical inputs are the decision on future beam energy, limited to 6.8 TeV in Run 3, and the assessment of the beam lifetime at the LHC during Run 3 with enhanced beam parameters enabled by the LIU upgrade. Alternative improvements of the proton cleaning performance are also under study, exploring for example changes of IR7 locally-generated dispersion or optics [Bruce *et al.* (2021)]. Key results are expected during 2023.

The betatron collimation system will additionally be upgraded to reduce its contribution to the machine impedance. New secondary collimators will replace 18 out of 22 TCS (see Table 1). The novel material molybdenum-graphite (MoGr) [Guardia-Valenzuela *et al.* (2018)], coated with a 6 μm layer of Mo, was chosen for the first upgrade during LS2. The improvement in surface resistivity from the present CFC secondary collimators reaches about a factor 100. The expected performance will be assessed in Run 3 thanks to the first-phase of the upgrade, where 8 new TCSs have already been installed during LS2. It is noted that the LS2 upgrade also involved the replacement of 4 primary collimators with a new design based on MoGr without coating, which would be at risk to be removed from primary beam losses impacting on the TCP surface. All new HL-LHC collimator embed in-jaw BPMs for faster alignment and local orbit monitoring [Dallocchio *et al.* (2011)].

4.4. *Crystal collimation of heavy-ion beams*

The collimation performance of heavy-ion beams in Run 3 relies on the crystal collimation scheme, shown schematically in Fig. 9. While the multi-stage cleaning requires several secondary collimators and absorbers, one single absorber per collimation plane would instead be sufficient, in theory, in a crystal-based collimation scheme. A bent crystal replaces the primary collimator and steers the impinging halo coherently on a single spot [Previtali (2010)]. Si crystals, 4 mm long and bent to a curvature radius of 80 m (producing a 50 μrad kick), are needed at the LHC [Mirarchi *et al.* (2017)]. Nuclear interactions are much reduced in this case [Redaelli *et al.* (2021b)], which translates into a reduction of dispersive losses downstream of the cleaning insertion. In practise, the crystal primary collimator will be inserted in the existing collimation hierarchy, slightly retracted with respect to the primary collimators that remain at their nominal positions, ensuring the passive machine protection in case of failures or orbit drifts opposite to the crystal [D'Andrea (2021)]. A minimum of 4 bent crystals is required

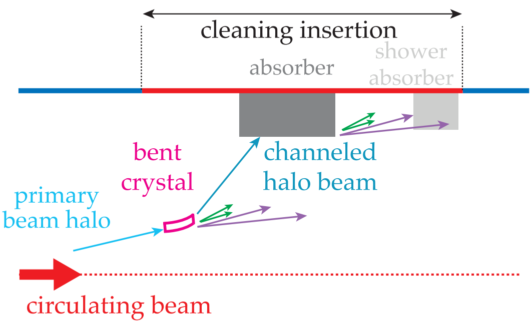

Fig. 9. The crystal collimation scheme.

for the horizontal and vertical collimation of both beams. Measurements performed in Run 2 demonstrated an improvement with Pb ion beams at 6.37 Z TeV by up to a factor 7, which is expected to be sufficient to achieve the HL-LHC goals if achieved in all beams and planes. The performance will be assessed in the first high-intensity Pb run in 2023.

4.5. *Active halo controls with hollow electron lenses*

Following the consistent observation of over-populated beam tails at the LHC [Valentino *et al.* (2013); Gorzawski *et al.* (2020)] and other colliders, hollow electron lenses (HELs) [Shiltsev (2016)] were integrated in the HL-LHC upgrade baseline to mitigate detrimental effects to the machine availability and safety from over-populated halos [Redaelli *et al.* (2021a)]. The HEL-based collimation scheme is shown in Fig. 10: a hollow electron beam, with inner radius below the aperture of the primary collimators, excited transverse particles outside the beam core. An ideal HEL generates zero field on the beam core, with no impact on the luminosity performance, while controlling the halo loss rates and populations over a broad range [Mirarchi *et al.* (2021)]. In reality, the field on the core cannot be null, and specific powering schemes are needed to drive the halo resonantly unstable. Various schemes are being studied and optimized for the HL-LHC operation, as shown for example in Fig. 11.

The construction of the HL-LHC lenses was planned as part of a Russian in-kind contribution. Following the critical international situation at the time of writing, it has became clear that the timeline for their deployment falls beyond the HL-LHC project duration, i.e. beyond the end of LS3. In these conditions, the lenses are no longer part of the HL-LHC baseline.

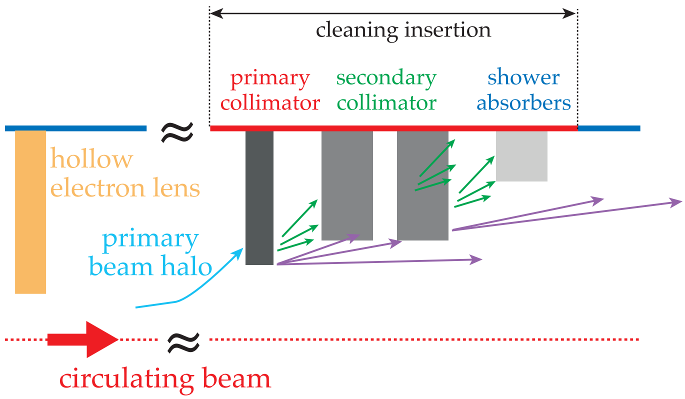

Fig. 10. Schematic view of the HEL collimation scheme: the HEL, typically located outside of the warm collimation region, actively controls the diffusion speed of particles at transverse amplitudes 1–2 σ below the TCP, without perturbing the core. The standard collimation system remains responsible of the safe disposal of the beam halo.

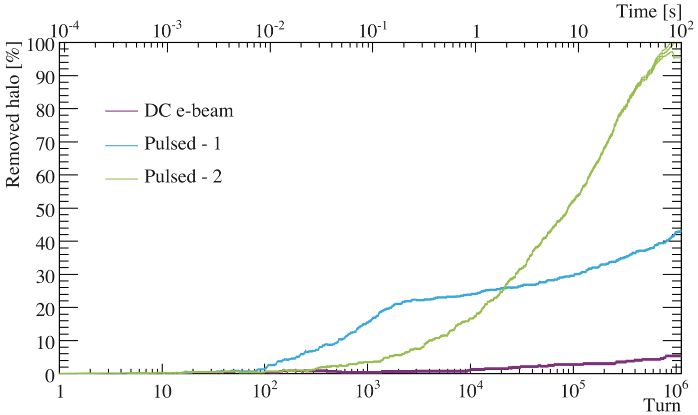

Fig. 11. Example of active halo depletion with HEL at the HL-LHC from [Mirarchi *et al.* (2021)] for different powering schemes for the electron beam: DC current (violet), random variations (green) and pulsed pattern with 9 turns ON and 14 turns OFF, as described in [Mirarchi *et al.* (2021)].

However, they are still pursued as a potential upgrade beyond the HL-LHC project, with earliest installation in LS4.

References

[Allonneau *et al.* (2018)] Allonneau, L., Boucly, C., Carlier, E., Ducimetiere, L., Magnin, N., Mottram, T., Senaj, V., Strobino, L., Rodziewicz, J., Van Trappen, P., Vez, B., and Voumard, N. (2018). LBDS Control Upgrade, `https://indico.cern.ch/event/784431/contributions/3263918/attachments/1790346/2916731/LBDS_Review_2019_LBDS_Controls_Upgrade_v2.pdf`.

[ATLAS Collaboration (2008)] The ATLAS experiment at the CERN Large Hadron Collider, *JINST* **3**, p. S08003.

[Barnes *et al.* (2017)] Barnes, M., Adraktas, A., Bregliozzi, G., Goddard, B., Ducimètiere, L., Salvant, B., Sestak, J., Vega Cid, L., Weterings, W., and Yin Vallgren, C. (2017). Operational experience of the upgraded LHC injection kicker magnets during Run 2 and future plans, *Journal of Physics: Conference Series* **874**, p. 012101, `https://doi.org/10.1088/1742-6596/874/1/012101`.

[Barnes *et al.* (2018)] Barnes, M., Bracco, C., Bregliozzi, G., Chmielinska, Ducimètiere, L., Goddard, B., Kramer, T., Neupert, H., Vega Cid, L., Vlachodimitropoulos, V., Weterings, W., and Yin Vallgren, C. (2018). An Upgraded LHC Injection Kicker Magnet, *"Proceedings of 9th International Particle Accelerator Conference", Vancouver, BC, Canada*, pp. 2632–2635, `http://cds.cern.ch/record/2672230/files/wepmk003.pdf`.

[Bruce *et al.* (2021)] Bruce, R., Maria, R. D., Giovannozzi, M., Mounet, N., and Redaelli, S. (2021). Optics configurations for improved machine impedance and cleaning performance of a multi-stage collimation insertion, *Proceedings of the 12th International Particle Accelerator Conference (IPAC'21): Campinas, Brazil, May 2021*, pp. 57–60, doi:doi: 10.18429/JACoW-IPAC2021-MOPAB006, `https://jacow.org/ipac2021/papers/MOPAB006.pdf`.

[Brüning *et al.* (2004)] Brüning, O. S., Collier, P., Lebrun, P., Myers, S., Ostojic, R., Poole, J., and P. Proudlock (editors), (CERN, Geneva, Switzerland, 2004). LHC design report v. 1: The LHC main ring, *CERN-2004-003-V1*.

[Brüning *et al.* (2004a)] Brüning, O., Collier, P., Lebrun, P., Meyers, S., Ostojic, R., Poole, J., and Proudlock, P. (2004a). LHC Design Report, **I**, pp. 417–440, `https://cds.cern.ch/record/782076?ln=fr`.

[Brüning *et al.* (2004b)] Brüning, O., Collier, P., Lebrun, P., Meyers, S., Ostojic, R., Poole, J., and Proudlock, P. (2004b). LHC Design Report, **I**, pp. 441–466, `https://cds.cern.ch/record/782076?ln=fr`.

[Carbajo Perez *et al.* (2021)] Carbajo Perez, D., Perillo-Marcone, A., Berthome, E., Bertone, C., Biancacci, N., Bracco, C., Bregliozzi, G., Bulat, B., Cadiou, C., Calviani, M., Cattenoz, G., Cherif, A., Costa Pinto, P., Dallocchio, A., Di Castro, M., Fessia, P., Frankl, M., Fuchs, J. F., Garcia Gavela, H., Gentini, L., Geisser, J. M., Gilardoni, S., Gonzalez De La Aleja Cabana, M. A., Grenard, J. L., Joly, S., Lechner, A., Lendaro, J., Maestre, J., Page, E., Perez Ornedo, M., Pugnat, D., Rigutto, E., Seidenbinder, R., Salvant, B., Sapountzis, A., Scibor, K., Sola Merino, J., Taborelli, M., Urrutia, E., Franqueira Ximenes, R., Vieille, A., Vollinger, C., and Yin Vallgren, C. (2021). New Generation CERN LHC Injection Dump – Assembly and Installation, *"Proceedings of 12th International Particle Accelerator Conference", Campinas, SP, Brasil*, pp. 3548–3551, https://cdsweb.cern.ch/record/2809172/files/document.pdf.

[Carra *et al.* (2014)] Carra, F. *et al.* (2014). Mechanical Engineering and Design of Novel Collimators for HL-LHC, in *5th International Particle Accelerator Conference*, p. MOPRO116, doi:10.18429/JACoW-IPAC2014-MOPRO116.

[CMS Collaboration (2008)] The CMS experiment at the CERN LHC, *JINST* **3**, p. S08004.

[Coupard *et al.* (2016)] Coupard, J., Damerau, H., Funken, A., Garoby, R., Gilardoni, S., Goddard, B., Hanke, K., Manglunki, D., Meddahi, M., Rumolo, G., Scrivens, R., and Chapochnikova, E. (2016). LHC Injectors Upgrade, Technical Design Report, Vol. II: Ions, Tech. Rep. CERN-ACC-2016-0041, CERN, Geneva, https://cds.cern.ch/record/2153863.

[Dallocchio *et al.* (2011)] Dallocchio, A., Boccard, C. B., Gasior, M., Carra, F., Bertarelli, A., Gentini, L., and Timmins, M. A. (2011). LHC Collimators with Embedded Beam Position Monitors: A New Advanced Mechanical Design, *Conf. Proc. C* **110904**, pp. 1611–1613.

[D'Andrea (2021)] *Applications of Crystal Collimation to the CERN Large Hadron Collider (LHC) and its High Luminosity Upgrade Project (HL-LHC)*, Ph.D. thesis, University of Padova, http://cds.cern.ch/record/2758839, presented 23 Feb 2021.

[Ducimètiere *et al.* (2003)] Ducimètiere, L., Garrel, N., and Barnes, M. (2003). The LHC Injection Kicker Magnet, *"Proceedings of the 2003 Particle Accelerator Conference", Portland, Oregon, US*, pp. 1162–1164, https://accelconf.web.cern.ch/p03/PAPERS/TPAE036.pdf.

[Ducimètiere and Senaj (2018)] Ducimètiere, L. and Senaj, V. (2018). LBDS Kickers: HW upgrade, https://indico.cern.ch/event/784431/contributions/3263915/attachments/1790226/2916321/HW_LBDS_review_05_Feb_2019.pdf.

[Gorzawski *et al.* (2020)] Gorzawski, A., Appleby, R., Giovannozzi, M., Mereghetti, A., Mirarchi, D., Redaelli, S. *et al.* (2020). Probing LHC halo dynamics using collimator loss rates at 6.5 TeV, *Phys. Rev. ST Accel. Beams* **23**, p. 044802.

[Guardia-Valenzuela *et al.* (2018)] Guardia-Valenzuela, J., Bertarelli, A., Carra, F., Mariani, N., Bizzaro, S., and Arenal, R. (2018). Development and properties of high thermal conductivity molybdenum carbide - graphite composites, *Carbon* **135**, pp. 72–84, doi:https://doi.org/10.1016/j.carbon.2018.04.010, http://www.sciencedirect.com/science/article/pii/S0008622318303555.

[Lechner *et al.* (2016)] Lechner, A., Barnes, M., Bartmann, W., Biancacci, N., Bracco, C., Bregliozzi, G., Butcher, M., Esteban Muller, J., Folch, R., Gentini, L., Gilardoni, S., Grudiev, A., Lamas Garcia, I., Losito, R., Masi, A., Metral, E., Perillo Marcone, A., Salvant, B., Taborelli, M., Uythoven, J., Vollenberg, W., and Yin Vallgren, C. (2016). TDI – Past Observations and Improvements for 2016, *"Proceedings 6th Evian Work-*

shop on LHC beam operation", Evian Les Bains, France, pp. 123–130, http://cds.cern.ch/record/2294666/files/1637016_123-130.pdf.

[Magnin *et al.* (2019)] Magnin, N., Bartmann, W., Bracco, C., Carlier, E., Gräwer, G., Mottram, T., Renner, E., Rodziewicz, P., Senaj, V., and Wiesner, C. (2019). Consolidation of Re-Triggering System of LHC Beam Dumping System at CERN, *"Proceedings of 17th International Conference on Accelerators and Large Experimental Physics Control Systems"*, pp. 412–416, https://cds.cern.ch/record/2778521/files/10.18429_JACoW-ICALEPCS2019-MOPHA088.pdf.

[Martin *et al.* (2021)] Martin, R., Jose, M., Kershaw, K., Calviani, M., Grenier, D., Maestre Herdia, J., Torregrosa, M., Claudio, L., Buonocore, L., Serrano, G., Matheson, E., and Sola Merino, J. (2021). Practical Challenges of the LHC Main Beam Dump Upgrades, https://cds.cern.ch/record/2786788.

[Mirarchi *et al.* (2021)] Mirarchi, D., Appleby, R., Bruce, R., Giovannozzi, M., Mereghetti, A., Redaelli, S., and Stancari, G. (2021). Nonlinear dynamics of proton beams with hollow electron lens in the CERN high-luminosity LHC, *Eur. Phys. J. Plus* **137**, p. 7, https://doi.org/10.1140/epjp/s13360-021-02201-5.

[Mirarchi *et al.* (2017)] Mirarchi, D., Hall, G., Redaelli, S., and Scandale, W. (2017). Design and implementation of a crystal collimation test stand at the large hadron collider, *The European Physical Journal C* **77**, 6, p. 424, doi:10.1140/epjc/s10052-017-4985-4, https://doi.org/10.1140/epjc/s10052-017-4985-4.

[Previtali (2010)] Previtali, V. (2010). *Performance evaluation of a crystal-enhanced collimation system for the LHC*, Ph.D. thesis, Ecole Polytechnique, Lausanne.

[Redaelli *et al.* (2020)] Redaelli, S., Bruce, R., Lechner, A., and Mereghetti, A. (2020). Chapter 5: Collimation system, *CERN Yellow Rep. Monogr.* **10**, pp. 87–114, doi:10.23731/CYRM-2020-0010.87.

[Redaelli *et al.* (2021a)] Redaelli, S., Appleby, R., Bruce, R., Brüning, O., Kolehmainen, A., Ferlin, G., Foussat, A., Giovannozzi, M., Hermes, P., Mirarchi, D., Perini, D., Rossi, A., and Stancari, G. (2021a). Hollow electron lenses for beam collimation at the High-Luminosity Large Hadron Collider (HL-LHC), *Journal of Instrumentation* **16**, 03, p. P03042, doi: 10.1088/1748-0221/16/03/p03042, https://doi.org/10.1088/1748-0221/16/03/p03042.

[Redaelli *et al.* (2021b)] Redaelli, S. *et al.* (2021b). First observation of ion beam channeling in bent crystals at multi-TeV energies, *Eur. Phys. J. C* **81**, 2, p. 142, doi:10.1140/epjc/s10052-021-08927-x.

[R. W. Assmann *et al.* (2006)] The Final Collimation System for the LHC, *Proc. of the European Particle Accelerator Conference 2006, Edinburgh, Scotland*, p. 986.

[Shiltsev (2016)] Shiltsev, V. D. (2016). *Electron Lenses for Super-Colliders*, Particle Acceleration and Detection (Springer), ISBN 978-1-4939-3315-0, 978-1-4939-3317-4, doi:10.1007/978-1-4939-3317-4.

[The ALICE Collaboration (2008)] The ALICE experiment at the CERN LHC, *Journal of Instrumentation* **3**, 08, p. S08002.

[The LHCb Collaboration (2008)] The LHCb Detector at the LHC, *Journal of Instrumentation* **3**, 08, p. S08005.

[Valentino *et al.* (2013)] Valentino, G., Aßmann, R., Bruce, R., Burkart, F., Previtali, V., Redaelli, S., Salvachua, B., Stancari, G., and Valishev, A. (2013). Beam diffusion measurements using collimator scans in the LHC, *Phys. Rev. ST Accel. Beams* **16**, p. 021003, doi:10.1103/PhysRevSTAB.16.021003.

[Valentino *et al.* (2017)] Valentino, G., Baud, G., Bruce, R., Gasior, M., Mereghetti, A., Mirarchi, D., Olexa, J., Redaelli, S., Salvachua, S., Valloni, A., and Wenninger, J. (2017). Final implementation, commissioning, and performance of embedded collimator beam position monitors in the large hadron collider, *Phys. Rev. Accel. Beams* **20**, p. 081002, doi:10.1103/PhysRevAccelBeams.20.081002, `https://link.aps.org/doi/10.1103/PhysRevAccelBeams.20.081002`.

[Vlachodimitropoulos *et al.* (2018)] Vlachodimitropoulos, V., Barnes, M., Ducimètiere, L., Vega Cid, L., and Weterings, W. (2018). Longitudinal Impedance Analysis of an Upgraded LHC Injection Kicker Magnet, *"Proceedings of 9th International Particle Accelerator Conference", Vancouver, BC, Canada*, pp. 2628–2631, `https://accelconf.web.cern.ch/ipac2018/papers/wepmk002.pdf`.